

# Dynamical lattice QCD thermodynamics and the $U(1)_A$ symmetry with domain wall fermions

Pavlos Vranas for the Columbia lattice group \*  
*University of Illinois at Urbana-Champaign, Urbana, IL 61801*

Results from numerical simulations of full, two flavor QCD thermodynamics at  $N_t = 4$  with domain wall fermions are presented. For the first time a numerical simulation of the full QCD phase transition displays a low temperature phase with spontaneous chiral symmetry breaking but intact flavor symmetry and a high temperature phase with the full  $SU(2) \times SU(2)$  chiral flavor symmetry. It is found that close to the transition in the high temperature phase the  $U(1)_A$  axial symmetry is broken only by a small amount. This result is of particular interest because of the connection between  $U(1)_A$  symmetry breaking and the expected order of the transition.

## I. INTRODUCTION

The upcoming RHIC experiments will reproduce the extreme conditions that existed in the early universe and it is hoped that the predicted QCD phase transition from hadronic matter to a quark-gluon plasma will be observed. The non-perturbative nature of these phenomena makes precise theoretical predictions difficult. Lattice gauge theory provides a first-principles approach to QCD thermodynamics and, in principle, a way to perform precise non-perturbative calculations of thermodynamic quantities at equilibrium. Quantities such as the value of the critical temperature, the width of the critical region and the order of the transition can then be used by phenomenological models to make contact with experiment. While great progress has been made since the inception of the lattice regulator 25 years ago [1] there remain very significant uncertainties that prevent these calculations from being viewed as unambiguous predictions of QCD. Since these calculations are computer simulations one could think that progress in this field is tied with progress in computer speeds. While this is partially true, it is not the real culprit especially given the fast growth in computer speeds during this period. The true reason lies at the most simple and fundamental level of the lattice theory.

When the first derivative of the fermion kinetic energy term is made into a lattice difference operator the number of light species multiplies by a factor of  $2^d$  where  $d$  is the dimension of space-time. This is the well known doubling problem and it turns out that at non-zero lattice spacing in order to remove the extra species and still have a local Lagrangian one has to compromise the global flavor chiral symmetries of the theory [2]. There are two popular methods to put fermions on the lattice: Wilson and staggered fermions. Both of these methods at finite lattice spacing  $a$  break the chiral symmetry. The chiral symmetry is recovered together with the Lorentz symmetry as the continuum limit  $a \rightarrow 0$  is taken. And here lies the problem. In a numerical simulation a decrease of the lattice spacing by a factor of 2 requires an increase in computation by a factor of  $2^{8-10}$  depending on the parameters. In order to control the amount of chiral symmetry breaking induced by the regulator prohibitively large computing resources are required. Clearly faster computers although one day may be able to overcome these large factors can not be the answer.

A way out of this forbidding state of affairs came from D. Kaplan [3] through an unexpected avenue. He formulated a new fermion lattice regulator with the name domain wall fermions (DWF). The first numerical simulations using DWF in vector gauge theories were done in [4] and were followed by [5], [6], [7], [8], [9], [10]. In this work the latest results from simulations of dynamical QCD thermodynamics are presented. Preliminary results of this work have already appeared in [6], [10]. For promising alternatives to domain wall fermion simulations see [11].

---

\*P. Chen, N. Christ, G. Fleming, A. Kaehler, C. Malureanu, R. Mawhinney, G. Siegert, C. Sui, P. Vranas, L. Wu, Y. Zhestkov

## II. DOMAIN WALL FERMIONS.

Domain wall fermions introduce an extra direction of space-time with size  $L_s$ . The fermion fields are five-dimensional while the gauge fields remain four-dimensional and couple the same way to all extra fermion degrees of freedom. The boundary conditions along the fifth direction are free (domain wall) and although the extra fermion degrees of freedom are heavy a light Dirac fermion surface mode develops on the boundaries with its positive chiral components exponentially bound on one wall and its negative components on the other. In the  $L_s \rightarrow \infty$  limit the mode is a massless Dirac fermion. At finite  $L_s$  the residual mixing introduces an exponentially small mass. Since these properties are maintained at any lattice spacing DWF provide a way of separating the recovery of the chiral symmetry from the recovery of the Lorentz symmetry. Now at a fixed lattice spacing the chiral symmetry can be recovered by increasing  $L_s$ . Unlike Wilson or staggered fermions the computing cost in recovery of the chiral symmetry is only linear in  $L_s$ ! These remarkable properties may bring within reach physically realistic studies of lattice QCD thermodynamics.

The subject of DWF has a large volume of work behind it. The reader is referred to [4] and references therein for an introduction. Here, the version of DWF as presented in [12] with the modifications in [4] is used. The theory has five parameters: the four-dimensional lattice volume  $V$ , the inverse gauge coupling squared  $\beta$ , a bare mass that explicitly mixes the two chiralities bound on the domain walls  $m_f$ , the number of sites of the fifth direction  $L_s$ , and a five-dimensional mass that can be thought of as the domain wall height  $m_0$ . The parameters  $m_f$ ,  $L_s$  and  $m_0$  set the bare quark mass. In free theory the bare quark mass  $m_{\text{eff}}$  is given by [4]:

$$m_{\text{eff}} = m_0(2 - m_0) [m_f + (1 - m_0)^{L_s}], \quad 0 < m_0 < 2 \quad (1)$$

There are many important theoretical issues regarding DWF. Perhaps the most crucial one relates to the localization of the chiral modes in the interacting theory. Does the localization remain exponential as in free theory or does it become power law? How does the decay rate depend on the lattice spacing? These questions were addressed in detail in [4] in the context of the two flavor Schwinger model. There it was found that the decay is exponential and that the decay rate becomes faster as the continuum limit is approached. The last result can be understood by a simple examination of eq. 1. In the interacting theory  $m_0$  will be renormalized and therefore optimum localization will be shifted away from  $m_0 = 1$ . However, even if  $m_0$  is adjusted to absorb this renormalization, optimal decay will not be possible since the optimal value for  $m_0$  will fluctuate from one background gauge field to the next. At strong coupling where the gauge field fluctuations are large the corresponding fluctuations in the optimal value of  $m_0$  will also be large and the decay rate will become slow. This scenario is reminiscent of the way the bare mass of Wilson type fermions is used to cancel the renormalization of the interacting theory. However, because the massless point changes from configuration to configuration masslessness can only be achieved up to order of the lattice spacing. Here the same is true but the fluctuations in mass are raised to the  $L_s$  power and therefore can be de-amplified by any amount for large enough  $L_s$ .

There is another related source of de-localizing effects. It has been shown that the transfer matrix along the extra direction for certain gauge field configurations can develop unit eigenvalues [13]. For such configurations the surface states completely de-localize. Although, the set of such configurations is of zero measure, configurations in their vicinity will produce poor localization. These configurations are special to the lattice since they allow the passage from one topological sector to another. Again, as the continuum limit is approached these configurations will have a negligible Boltzmann weight and their de-localizing effects will diminish.

Another issue relates to the positivity of the transfer matrix along the fifth direction. Details regarding this can be found in [14]. Here, it suffices to mention that if  $L_s$  is kept even and if all Green's functions are extracted from sites along the fifth direction that have a distance from the boundaries of an even number of sites the relevant transfer matrix is the square of the single step one and is therefore positive.

Finally the number of light flavors of the free theory depends on  $m_0$ . For example if  $0 < m_0 < 2$  the theory has one light flavor but if  $2 < m_0 < 4$  the theory has four light flavors. These  $m_0$  ranges are modified in the interacting theory and one should make sure that the needed number of flavors is produced [7], [6].

### III. TWO FLAVOR SCHWINGER MODEL.

The two flavor Schwinger model was simulated numerically in [4]. If the chiral symmetries of the massless model are intact, the chiral condensate will have a zero vacuum expectation value,  $\langle \bar{\Psi}\Psi \rangle = 0$  at all couplings. Therefore, the deviation of  $\langle \bar{\Psi}\Psi \rangle$  from zero can serve as a measure of the amount of chiral symmetry breaking induced by the regulator. In figure 1 the results from these simulations are presented.

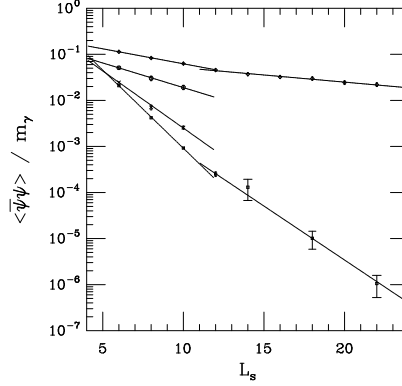


FIG. 1. The chiral condensate normalized by the photon mass for  $m_f = 0$ ,  $m_0 = 0.9$ . From top to bottom the lines correspond to lattice spacing  $a$  of  $1/6, 1/8, 1/10$  and  $1/12$ . The solid lines are fits to  $c_0 e^{-c_1 L_s}$ .

There are three observations that can be made from this figure:

- 1) For each lattice spacing there are two different decay rates. In [4] the fast rate was related to the physics of the zero topological sector while the slow rate was related to the physics of topology changing configurations.
- 2) Fits to an exponential decay form  $c_0 e^{-c_1 L_s}$  have  $\chi^2$  per degree of freedom around one indicating that the localization of the light states in the interacting theory is consistent with exponential decay. Also, power law behavior can be excluded with some confidence for the  $a = 1/12$  data since a power law fit has a  $\chi^2$  per degree of freedom of 32.
- 3) The decay rates become faster as the lattice spacing is decreased. This is a key feature that makes DWF a viable lattice fermion regulator.

### IV. QUENCHED QCD.

Before DWF can be used in QCD an analysis similar to the one for the Schwinger model must be done in order to map the parameter space. Below the results from such an analysis using quenched QCD are presented. Preliminary results can be found in [7], [8].

As mentioned in section II  $m_0$  controls the number of light flavors. Since this parameter is renormalized, it is important to understand which ranges correspond to different flavor sectors. In figure 2a  $\langle \bar{\Psi}\Psi \rangle$  is plotted as a function of  $m_0$ . Three regions can be distinguished:  $\langle \bar{\Psi}\Psi \rangle$  is zero for  $m_0 < 1$ , it has a value around 0.001 for  $1 < m_0 < 2.5$  while it has a value that is four times larger for  $2.5 < m_0 < 4.0$ . Therefore, these three regions correspond to a zero, two and eight flavor theory (for algorithmic reasons only an even number of flavors is simulated; had it not been for this restriction the three regions would correspond to zero, one and four flavors).

In order to investigate the  $L_s$  dependence of the theory the pion mass  $m_\pi$  is measured for several values of  $m_f$  at fixed  $L_s$  and  $m_0$  for  $\beta = 5.7$  on an  $8^3 \times 32$  lattice. Its value is then extrapolated to zero quark mass. This exercise is repeated for several values of  $L_s$ . The  $m_f = 0$  extrapolated value as a function of  $L_s$  is shown in figure 2b for  $m_0 = 1.65$ . The solid line is a fit to  $c_0 + c_1 e^{-c_2 L_s}$ . The fit has  $\chi^2/\text{d.o.f.} \approx 1$  indicating that the localization is consistent with exponential decay. The constant part of the fit is due to finite volume. On a finite box of size  $L$  and periodic boundary conditions the longest correlation length is  $L/2$  and therefore the smallest mass should be  $\approx 2/L$ . In this case  $m_\pi(m_f = 0, L_s = \infty) \approx 0.22 \approx 2/8$ . That this is indeed a finite volume effect was supported by a second simulation on a  $16^3 \times 32$  lattice.

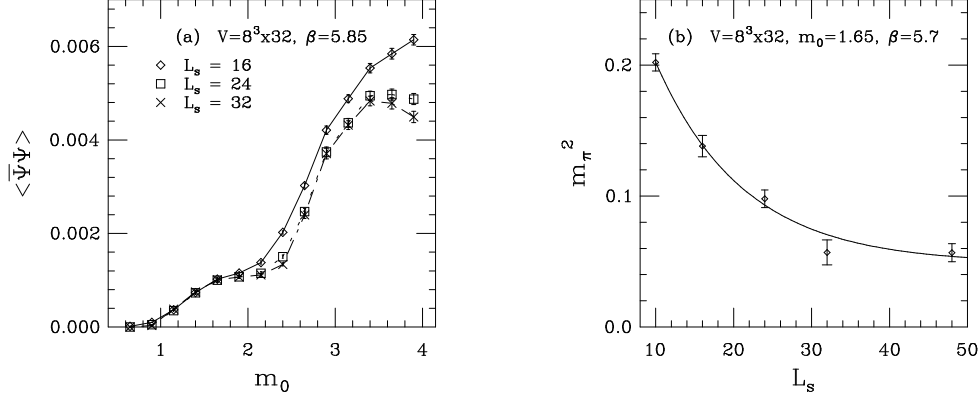


FIG. 2. (a)  $\langle \bar{\Psi}\Psi \rangle$  extrapolated to  $m_f = 0$  vs.  $m_0$  for various  $L_s$ . (b)  $m_\pi^2$  extrapolated to  $m_f = 0$  vs.  $L_s$ .

Finally, the rho and nucleon masses were measured for several  $m_f$  and  $L_s$ . Their  $m_f = 0$  extrapolated values showed almost no dependence on  $L_s$  for  $10 \leq L_s$ . The nucleon to rho mass ratio was found to be  $m_N/m_\rho = 1.508(65)$  to be compared with the physical value 1.221(2). The discrepancy is expected since the lattice spacing is rather large,  $a \approx 0.2fm$ , and the box size only marginally large  $1.6fm$ . Given the modest volume size these results compare favorably with previous quenched QCD results using Wilson and staggered fermions at larger volumes.

## V. DYNAMICAL QCD THERMODYNAMICS.

With this ground work in hand dynamical QCD thermodynamics can be investigated. The first exploratory work is done on small lattices of size  $8^3 \times 4$ . Preliminary results have been presented in [6]. In figure 3a  $\langle \bar{\Psi}\Psi \rangle$  as a function of  $\beta$  is shown for a fixed  $L_s$  and  $m_f$  at  $m_0 = 1.9$ . A rapid crossover is observed indicating the presence of a phase transition. To confirm that indeed there are two phases  $\langle \bar{\Psi}\Psi \rangle$  is plotted in figure 3b as a function of  $m_f$  at  $L_s = 16$  for  $\beta = 5.20$  below the transition and  $\beta = 5.45$  above. Clearly below the transition  $\langle \bar{\Psi}\Psi \rangle$  extrapolates to a non zero value indicating spontaneous breaking of the  $SU(2) \times SU(2)$  chiral symmetry down to  $SU(2)$  flavor. Because the Lagrangian is explicitly symmetric under the  $SU(2)$  flavor there are three degenerate Goldstone pions. Above the transition  $\langle \bar{\Psi}\Psi \rangle$  extrapolates to a non zero but very small value (which could be further reduced by increasing  $L_s$ ) indicating that the full  $SU(2) \times SU(2)$  chiral symmetry is essentially restored. This illustrates the unique properties of DWF.

To further study the properties of the dynamical theory  $\langle \bar{\Psi}\Psi \rangle$  is plotted as a function of  $L_s$  for  $m_f = 0.02$ ,  $m_0 = 1.9$  both below ( $\beta = 5.20$ ) and above ( $\beta = 5.45$ ) the transition in figure 4a. The fits are of the form  $c_0 + c_1 e^{-c_2 L_s}$ . The constant term is the value of the condensate at the non-zero mass  $m_f$ . The  $\chi^2/\text{d.o.f.}$  is small indicating that the localization of the dynamical theory is consistent with exponential. As seen in the Schwinger model the decay rate becomes faster as the lattice spacing is made smaller (increasing  $\beta$ ). At  $\beta = 5.45$  the  $L_s = \infty$  value of  $\langle \bar{\Psi}\Psi \rangle$  is already approached to within a few percent at  $L_s = 16$  while at  $\beta = 5.20$  a larger  $L_s$  is needed. Although these results are encouraging it must be stressed out that at this large lattice spacing other observables may have different decay characteristics.

Finally it is important to investigate the behavior of the phase transition as a function of  $m_0$ . In figure 4b the Wilson line is shown as a function of  $\beta$  for various  $m_0$ . A similar plot has also been obtained for  $\langle \bar{\Psi}\Psi \rangle$  but because the wavefunction renormalization of the fermion field depends on  $m_0$ , it is hard to display in a single figure. From left to right the figure corresponds to  $m_0 = 2.15, 1.90, 1.80, 1.65$ . The qualitative features of these curves are similar but the critical value of  $\beta$  is a strong function of  $m_0$ . This is not surprising since  $\beta$  is a bare parameter. One observes that as  $m_0$  is reduced the critical  $\beta$  approaches the quenched value  $\beta_c = 5.7$  indicating that the regime of zero flavors is approached. The role of  $m_0$  in thermodynamics should be studied with some caution. For example, from free field

studies the range of small momenta accessible to the light flavor is restricted if  $m_0$  is set close to its lower bound for one flavor physics. Similar effects can occur if  $m_0$  is set close to its upper bound for one flavor physics. Since such a restriction may affect the thermodynamics one should set  $m_0$  somewhere in the middle of the allowed range.

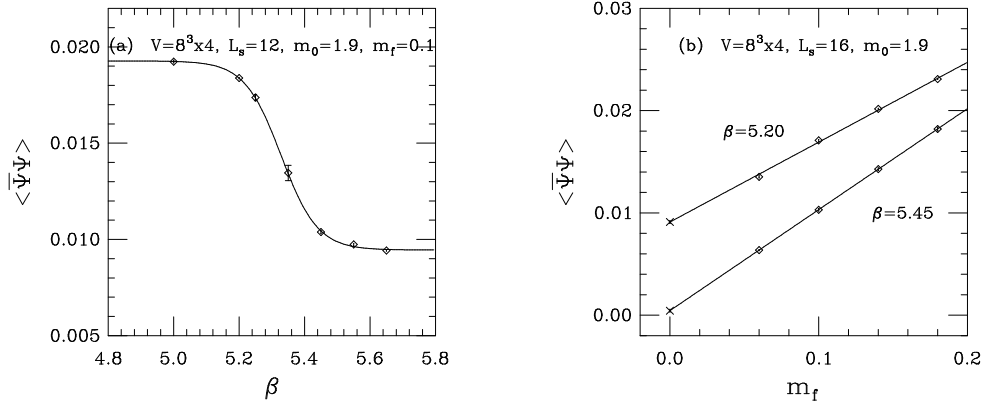


FIG. 3.  $\langle \bar{\Psi}\Psi \rangle$  around the QCD finite temperature phase transition.

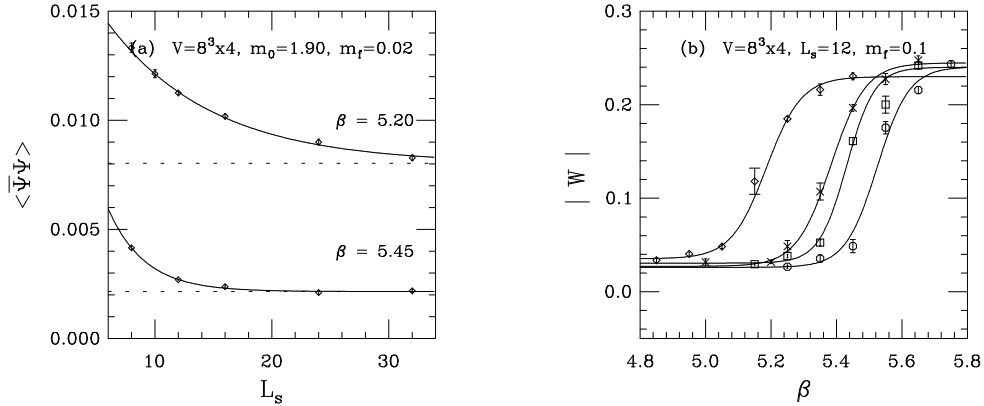


FIG. 4. (a)  $\langle \bar{\Psi}\Psi \rangle$  vs.  $L_s$  below and above the transition. (b) The Wilson line  $|W|$  vs.  $\beta$  for various  $m_0$ .

## VI. THE $U(1)_A$ SYMMETRY JUST ABOVE THE QCD DECONFINING TRANSITION.

If the  $U(1)_A$  symmetry above but close to the deconfining phase transition is broken the transition is expected to be second order while if it is not broken or only softly broken the transition may be first order [15]. This important issue can be investigated by direct lattice QCD simulations just above the transition. Using staggered fermions [16] it was not possible to draw unequivocal conclusions mainly because staggered fermions may not produce the zero mode effects necessary for anomalous breaking of  $U(1)_A$  [17], [18]. On the other hand DWF are known to possess exact and robust zero modes in the  $L_s = \infty$  limit [13]. In [19] it was shown that for classical instanton backgrounds these properties are maintained with high accuracy even at finite  $L_s \approx 10$ . In order to confirm the presence of zero modes in a situation with quantum fluctuations  $\langle \bar{\Psi}\Psi \rangle$  versus  $m_f$  from a numerical simulation of quenched QCD just above the transition is plotted in figure 5a. Since in the quenched approximation the fermionic determinant is set to one, the zero mode effects are not suppressed and  $\langle \bar{\Psi}\Psi \rangle$  diverges as  $1/m_f$ .

Having established that DWF exhibit the desired zero mode effects the  $U(1)_A$  symmetry is probed by numerical simulations of full QCD using DWF on a large lattice above the deconfining transition. The difference  $m_\delta - m_\pi$  of the screening masses of the delta and pion particles is used as a measure of anomalous symmetry breaking. The screening masses are measured from the exponential fall-off of the relevant two point Green's function along a spatial

direction. Since the delta and pion Green's function are related by a  $U(1)_A$  transformation  $m_\delta - m_\pi$  should be zero in the zero mass limit if the symmetry is not broken and non-zero otherwise. In figure 5b  $m_\delta - m_\pi$  versus  $m_f$  is shown for  $\beta = 5.45$  and  $\beta = 5.40$  on a  $16^3 \times 4$  lattice with  $L_s = 16$  and  $m_0 = 1.9$ . The critical  $\beta$  is around 5.325. The lines are fits to  $c_0 + c_2 m_f^2$  and have  $\chi^2/\text{d.o.f.} \approx 1$ . The absence of a linear term indicates that chiral symmetry is effectively restored. The  $m_f = 0$  extrapolated values are 0.087(17) at  $\beta = 5.40$  and 0.031(9) at  $\beta = 5.45$ . Although both are not zero their value is small when compared with  $m_\delta$  and  $m_\pi$  which are  $\approx 1.3$ . Universality arguments require that if the QCD phase transition is to be second order, the anomalous  $U(1)_A$  must be broken. It is an open question as to whether the small size of the  $U(1)_A$  symmetry breaking seen here is sufficient to support this theoretical prediction that the two-flavor QCD phase transition is second order [15].

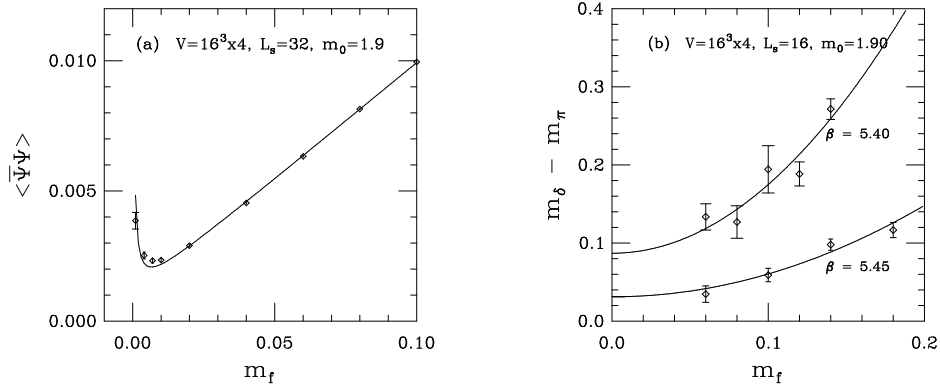


FIG. 5. (a)  $\langle \bar{\Psi}\Psi \rangle$  in quenched QCD just above the transition. (b)  $m_\delta - m_\pi$  in dynamical QCD just above the transition.

## VII. THE CHARACTER OF THE QCD PHASE TRANSITION.

In order to determine the critical temperature and investigate the width of the critical region and the order of the transition, simulations of full QCD with DWF on  $16^3 \times 4$  lattices close to the transition are performed for  $m_0 = 1.9$ ,  $m_f = 0.02$  and  $L_s = 24$ . The chiral condensate is plotted as a function of  $\beta$  in figure 6. For each  $\beta$  two separate simulations are done one with an ordered initial configuration (diamonds) and one with a disordered one (crosses).

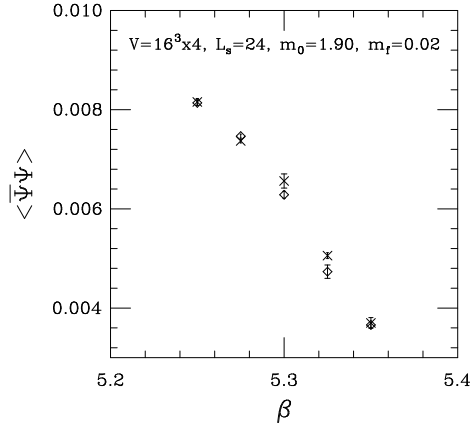


FIG. 6.  $\langle \bar{\Psi}\Psi \rangle$  vs.  $\beta$  on a  $16^3 \times 4$  lattice with  $m_0 = 1.9$ ,  $m_f = 0.02$  and  $L_s = 24$ .

A zero temperature dynamical simulation on an  $8^3 \times 32$  lattice at  $\beta = 5.325$  with  $m_0 = 1.9$ ,  $m_f = 0.02$  and  $L_s = 24$  is done in order to set the scale close to the transition. The valence extrapolated  $\rho$  mass is found to be  $m_\rho = 1.198(57)$ . If it is used to set the scale it results to a critical temperature  $T_c \approx 161\text{MeV}$ . The pion mass at  $m_f = 0.02$  is  $m_\pi \approx 412\text{MeV}$ . Further analysis attributes this large value to finite  $L_s$  effects. This is under current investigation.

Finally, from figure 6 one can see that the ordered and disordered points at  $\beta = 5.325$  disagree even though each

was determined after 400 thermalization sweeps were discarded. These small discrepancies visible for  $\beta = 5.3$  and 5.325 suggest the presence of a critical region and indicate the need for collecting more statistics, a process currently underway. Also,  $m_\pi$  must be reduced before the order of the transition can be identified. This is currently in progress.

## VIII. CONCLUSIONS.

A novel lattice fermion regulator, domain wall fermions, was used to study QCD thermodynamics. For the first time, this regulator offers the possibility to control the notorious lattice chiral/flavor asymmetries that have impeded numerical studies of QCD thermodynamics. The  $U(1)_A$  symmetry above the deconfining transition was found to be broken only by a small amount. The critical temperature for the transition was calculated and was found to be in agreement with previous estimates. Detailed studies of the transition region are currently underway with the hope that a consistent picture of the order of the transition and the relatively small  $U(1)_A$  breaking will emerge. However, smaller pion masses are needed before any conclusions can be drawn and such work is now underway.

## IX. ACKNOWLEDGMENTS.

The simulations were done on the 400 Gflops QCDSF supercomputer [20] at Columbia. This research was partially supported by DOE under grant # DE-FG02-92ER40699 and for PV partially under grant # NSF-PHY96-05199.

- 
- [1] K.G. Wilson, Phys. Rev. **D10** (1974) 2445.
  - [2] H.B. Nielsen and M. Ninomiya Nucl. Phys. bf B185 (1981) 20.
  - [3] D.B. Kaplan, Phys. Lett. **B288** (1992) 342; Nucl. Phys. **B30** (Proc. Suppl.) (1993) 597.
  - [4] P.M. Vranas, LATTICE 96, Nucl. Phys. **B53** (Proc. Suppl.) (1997) 278; P.M. Vranas Phys. Rev. **D57** (1998) 1415.
  - [5] T. Blum and A. Soni, Phys. Rev. **D56** (1997) 174; Phys. Rev. Lett. **79** (1997) 3595.
  - [6] P. Chen, N. Christ, G. Fleming, A. Kaehler, C. Malureanu, R. Mawhinney, G. Siebert, C. Sui, P. Vranas, and Y. Zhestkov, contribution to LATTICE 98, hep-lat/9809159.
  - [7] P. Chen, N. Christ, G. Fleming, A. Kaehler, C. Malureanu, R. Mawhinney, G. Siebert, C. Sui, P. Vranas, and Y. Zhestkov, contribution to LATTICE 98, hep-lat/9811026.
  - [8] P. Chen, N. Christ, G. Fleming, A. Kaehler, C. Malureanu, R. Mawhinney, G. Siebert, C. Sui, P. Vranas, and Y. Zhestkov, contribution to LATTICE 98, hep-lat/9811013.
  - [9] P. Chen, N. Christ, G. Fleming, A. Kaehler, C. Malureanu, R. Mawhinney, G. Siebert, C. Sui, P. Vranas, and Y. Zhestkov, contribution to LATTICE 98, talk by A. Kaehler.
  - [10] P. Chen, N. Christ, G. Fleming, A. Kaehler, C. Malureanu, R. Mawhinney, G. Siebert, C. Sui, P. Vranas, and Y. Zhestkov, contribution to ICHEP 98, hep-lat/9812011.
  - [11] H. Neuberger, Phys. Rev. **D57** (1998) 5417; Phys. Lett. **B417** 141 (1998); Phys. Rev. Lett. **81** (1998) 4060; hep-lat/9901003; U.M. Heller, R. Edwards and R. Narayanan hep-lat/9807017; hep-lat/9811030; C. Lieu, hep-lat/9811008.
  - [12] V. Furman, Y. Shamir, Nucl. Phys. **B439** (1995) 54.
  - [13] R. Narayanan, H. Neuberger, Phys. Lett. **B302** (1993) 62; Phys. Rev. Lett. **71** (1993) 3251; Nucl. Phys. **B412** (1994) 574; Nucl. Phys. **B443** (1995) 305.
  - [14] P. Chen, N. Christ, G. Fleming, A. Kaehler, C. Malureanu, R. Mawhinney, G. Siebert, C. Sui, P. Vranas, and Y. Zhestkov, in preparation.
  - [15] R. Pizarski and F. Wilczek, Phys. Rev. **D29** (1984) 338.
  - [16] S. Chandrasekharan, D. Chen, N.H. Christ, W. Lee, R. Mawhinney, and P.M. Vranas, CU-TP-902, hep-lat 9807018.
  - [17] J.B. Kogut, J.F. Lagae, D. K. Sinclair, hep-lat/9801020.
  - [18] A. Kaehler in preparation.
  - [19] P. Chen, N. Christ, G. Fleming, A. Kaehler, C. Malureanu, R. Mawhinney, G. Siebert, C. Sui, P. Vranas, and Y. Zhestkov, Phys. Rev. **D59** (1999) 054508.
  - [20] D. Chen, P. Chen, N. Christ, R. Edwards, G. Fleming, A. Gara, S. Hansen, C. Jung, A. Kaehler, A. Kennedy, G. Kilcup, Y. Luo, C. Malureanu, R. Mawhinney, J. Parsons, C. Sui, P. Vranas, and Y. Zhestkov, contribution to LATTICE 98, hep-lat/9810004.